

Spectroscopic analysis of poly(methyl methacrylate)/alumina polymer nanocomposites prepared by *in situ* (bulk) polymerization

Wantinee Viratyaporn · Richard L. Lehman

Received: 13 April 2010 / Accepted: 29 May 2010 / Published online: 22 June 2010
© Springer Science+Business Media, LLC 2010

Abstract Poly(methyl methacrylate) polymer nanocomposites were prepared by *in situ* bulk free radical polymerization. To ensure high-quality dispersion of the oxide nanoparticles, some composites were prepared from nanoparticles predispersed in propylene glycol methyl ether acetate (PGMEA). The degree to which this additional dispersing medium interacted with the aluminum oxide nanoparticle was studied by attenuated total reflectance (ATR-FTIR), which confirmed secondary bonding and ionic interaction across the particle/dispersing medium interface. Additionally, the effect of the dispersing medium and the nanoparticles on the degree of monomer conversion was determined by Raman spectroscopy. In the presence of oxide nanoparticles alone, the active surface of the nanoparticles traps propagating radicals which significantly reduces monomer conversion. Conversely, the degree of monomer conversion is enhanced in composites containing predispersing nanoparticles, apparently by passivation/functionalization of the oxide surface by the PGMEA.

Introduction

The exceptional synergetic properties of certain polymer nanocomposites have recently drawn lots of attention both in academia as well as in industry. Nevertheless, due to surface energy differences between hydrophilic nanoparticles and hydrophobic polymers, the fabrication of polymer nanocomposite with optimum properties is a challenging

task. Surface modification of nanoparticles is an effective approach to overcome the incompatibility and improve interactions between polymer and nanoparticles which consequently enhance nanoparticle dispersion as well as properties of polymer nanocomposites [1, 2]. In addition, a variety of processing techniques have been performed to produce high-quality and uniform properties of the composite materials [1–6]. One of the most economical ways to commercially produce polymer nanocomposites is by melt mixing. However, due to the high viscosity of most polymer melts, this dispersion method is not as effective as predispersing the nanoparticles in a low-viscosity medium, e.g., the monomer or other functionalizing fluid, followed by *in situ* polymerization [7].

Bulk polymerization is well-known as a highly exothermic reaction which leads to rapid polymerization due to low transport requirements and poor heat dissipation. This autoacceleration process is also known as the gel, or Trommsdorf, effect which can have the additional undesirable side effect of trapping unpolymerized monomers and propagating radicals inside the polymer chain clusters [8, 9]. The unreacted monomers lead to poor properties and side effects in the final products which are not acceptable in many applications, particularly in the medical field. On the other hand, complete conversion of methyl methacrylate monomer has been reported in certain polymerization processes [10]. The percent of monomer conversion can be determined by many techniques such as chromatography (HPLC and GPC) [11, 12] and spectroscopy (NMR, FTIR, and Raman spectroscopy) [13–15]. FTIR and Raman spectroscopy are widely used in the medical field for the determination of degree of monomer conversion in dental composites [15–17] and bone cement [18, 19] due to convenience and simplicity of the technique that can be performed on site.

W. Viratyaporn · R. L. Lehman (✉)
AMIPP Advanced Polymer Center, School of Engineering,
Rutgers, The State University of New Jersey, Piscataway,
NJ 08854-8065, USA
e-mail: rlehman@rutgers.edu

The main purpose of this work was to use Raman spectroscopy to quantify the degree of polymerization in poly(methyl methacrylate)/aluminum oxide nanocomposites. Of particular interest is the role of particle dispersion facilitated by propylene glycol methyl ether acetate (PGMEA) used as a functionalizing agent and as a medium for predispersion of the nanoparticles. Specifically, we were interested in the role of the glycol molecule on polymerization, which has the particular capability to bind onto the nanoparticle surface and consequently affect the polymerization process.

Experimental procedure

In situ polymerization of PMMA/alumina nanocomposites

MMA monomer (Acros Organics) was purified by passing through a column packed with aluminum oxide to remove the inhibitor by adsorption. Then, a PMMA syrup was prepared by combining PMMA beads purchased from Polysciences, Inc. (15 vol%) with purified MMA (85 vol%) and stirred for 24 h at room temperature. Aluminum oxide nanoparticles (detail in Table 1) were dispersed in the syrup by ultra-sonication for 20 min at 35 W for the total energy of 420 kJ followed by the addition of AIBN (1 wt%) with magnetic stirrer for 5 min. Subsequently, the mixture was degassed under mechanical vacuum for 5 min. Sheet molds, prepared from two glass plates sealed with window spacing tape was filled with the degassed mixture and placed into an isothermal water bath at 50 °C for 24 h to polymerize the composite and to develop initial strength. A final stage of polymerization was conducted at 95 °C for 1 h. Each type of nanoparticles was varied with three concentrations. Detailed quantities of the polymer nanocomposites are listed in Table 2. The high surface energy of nanoparticles can lead to the formation of particle agglomerates. The as-received predispersed nanoparticle slurries were cloudy, indicating the presence of light-scattering agglomerates. These agglomerates, which resisted dispersion during subsequent ultrasonication, generated light scattering and opacity in the fabricated composites.

Table 1 Information of nanoparticles

Trade name	Oxide	v/o in PGMEA	d^a (nm)	Surface area (m^2/g)	Geometry
NanoTek® Aluminum oxide (dry powder)	Al_2O_3	–	45	32–40	Sphere
NanoArc® R1130PMA	Al_2O_3	10.35	20	83	Sphere
NanoDur® X1130PMA	Al_2O_3	21.23	45	32–40	Sphere

Note: All particles were synthesized by a plasma-based vapor process

^a Mean particle size

Table 2 Composition info

Systems	Compositions		
	Particle (v/o)	PMMA (v/o)	PGMEA (v/o)
PMMA	0	100	0
PMMA/PGMEA	0	99	1
	0	97	3
	0	95	5
	0	93	7
PMMA/ Al_2O_3 (dry powder, 45 nm)	1	99	0
PMMA/FG- Al_2O_3 (20 nm)	0.49	95.25	4.26
	0.94	90.90	8.16
	1.36	86.88	11.76
PMMA/FG- Al_2O_3 (45 nm)	0.50	97.63	1.87
	0.99	95.34	3.67
	1.46	93.14	5.40

Characterization

Infrared spectra were collected by a diamond crystal ATR-FTIR from Bruker. Each spectrum was scanned on average of 100 scans with the scan resolution of 4 cm^{-1} . All spectra were analyzed with KnowItAll software from BioRad. For analysis of predispersed nanoparticles, the excess PGMEA was first eliminated. The predispersed particles were weighed into an aluminum pan and dried under isothermal vacuum at 50 °C for at least 19 h.

Raman shift spectra were collected with Renishaw inVia Raman microscope in the spectrum range of 200–3200 cm^{-1} . The excitation wavelength was 785 nm, and magnification was 50 \times resulting approximately 1 μm of beam diameter on the sample surface. A grating beam path of 1200 L/mm was used. Specimens were prepared from molded composites by cutting small pieces from the sheet and placing the specimen under the Raman microscope such that the beam was incident with the smooth-molded surface. Each spectrum accumulation was replicated 16 times and averaged to enhance accuracy and increase signal-to-noise ratio. Subsequently, data were analyzed with Wire2 (SP9), software supplied by Renishaw.

Results and discussions

Interfacial interaction of predispersed nanoparticles

Surface of metal oxides are generally covered with hydroxyl groups ($-OH$) as a result of the interaction between the metal oxide and surrounding chemical moieties, which can vary in type but are often of alcohol or OH character. Regardless of how they originate, the pure O–H stretching, without any secondary bonding between the neighboring atoms, produces an absorption band near 3650 cm^{-1} [20]. Additionally, the hydroxyl group can interact with the other hydroxyl groups via secondary bonding, an effect that shifts and broadens the O–H stretching peak toward lower frequencies. As compared to the FTIR spectra of PGMEA and aluminum oxide, the spectrum of absorbed PGMEA indicates that the interactions of between metal oxide and PGMEA exist (Fig. 1). A typical interaction between surface hydroxyl and polar substance is acid–base interaction via secondary bonding [21, 22] which is expected to occur at the high electron density sites of the PGMEA molecule. Such interaction is evidenced by the shift of the hydroxyl group absorption

band and its related counter interactions, which are carbonyl (from 1734 to 1731 cm^{-1}) and ether (from 1113 to 1103 cm^{-1}) vibrations, toward the lower frequency. As PGMEA molecules approach and bind onto the aluminum oxide particles, not only are vibrations of the bound section altered but also the unreacted segments of the molecules. The C–H stretching peak (2800 – 3050 cm^{-1} region) changes its shape and intensity as PGMEA molecule is bound onto the particle surface which could be a result of electron extraction and the change in the molecular environment. The acid–base interactions between PGMEA and aluminum oxide nanoparticles are illustrated in Scheme 1.

Ester compounds can undergo hydrolysis reactions upon interaction with surface hydroxyl group and form carboxylate ($-COO-$) end groups [21]. Three binding configurations between carboxylate group and metal oxide surface have been proposed—unidentate, bridging bidentate, and chelating bidentate [23–26]. These ionic binding structures between carboxylate anion and aluminum oxide surface are illustrated in Scheme 2. Each structure can be distinguished by the wave number differences between symmetric and asymmetric stretching of the carboxylate anion. The vibrational frequency of asymmetric stretching in the case of unidentate configuration is higher than that of bidentate one and vice versa for symmetric stretching. Consequently, the extent of frequency differences ($\Delta\nu_{a-s}$) is higher in unidentate configuration than bidentate one. Bidentate species were reported to behave as either bridging or chelating structures where the $\Delta\nu_{a-s}$ is smaller in the chelating structure.

The broad vibrational frequency response of the complex bidentate structure is evidenced by the broad peak at 1500 – 1600 cm^{-1} , as shown in Fig. 1b and is an indicator of the hydrolysis reaction of PGMEA molecules. In this work, only two types of complex structure are detected, the unidentate and the bridging bidentate structures. Although the COO– asymmetric stretching of unidentate ($\sim 1720\text{ cm}^{-1}$) is not visible due to the location of the expected COO– asymmetric stretching (it could also simply be overpowered by the large C=O stretching peak), the small peak at 1295 cm^{-1} which belongs to the symmetric one is clearly observed.

Effect of nanoparticles on extent of polymerization

Raman spectroscopy is suitable for analysis of polarized molecules; therefore, one interesting application of this feature is to investigate the percent conversion of monomer in the polymerization process [27–29]. Methyl methacrylate monomer has an unsaturated double bond (C=C) which will open upon polymerization to form long polymer chains, while the carbonyl group (C=O) remains unchanged. The vibrational frequencies of C=C and C=O are 1640

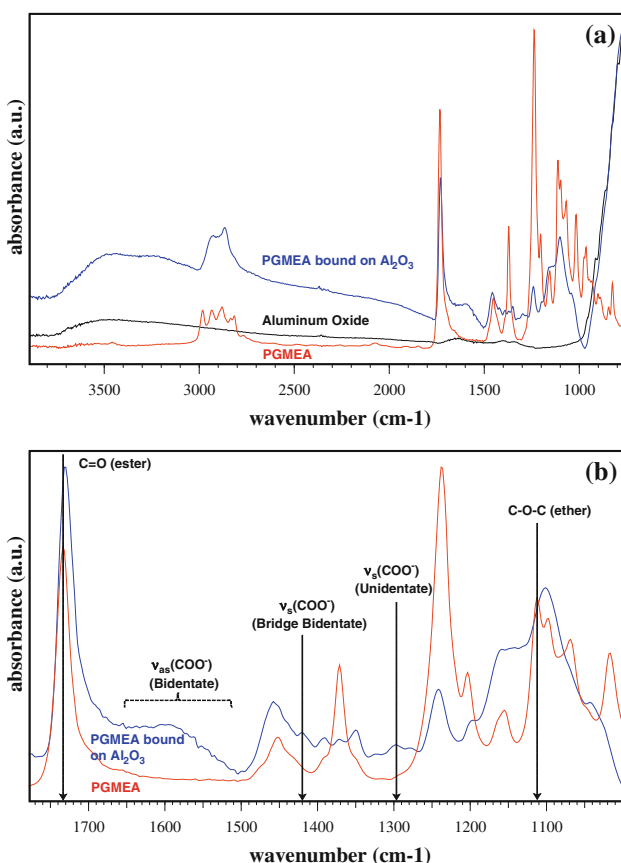
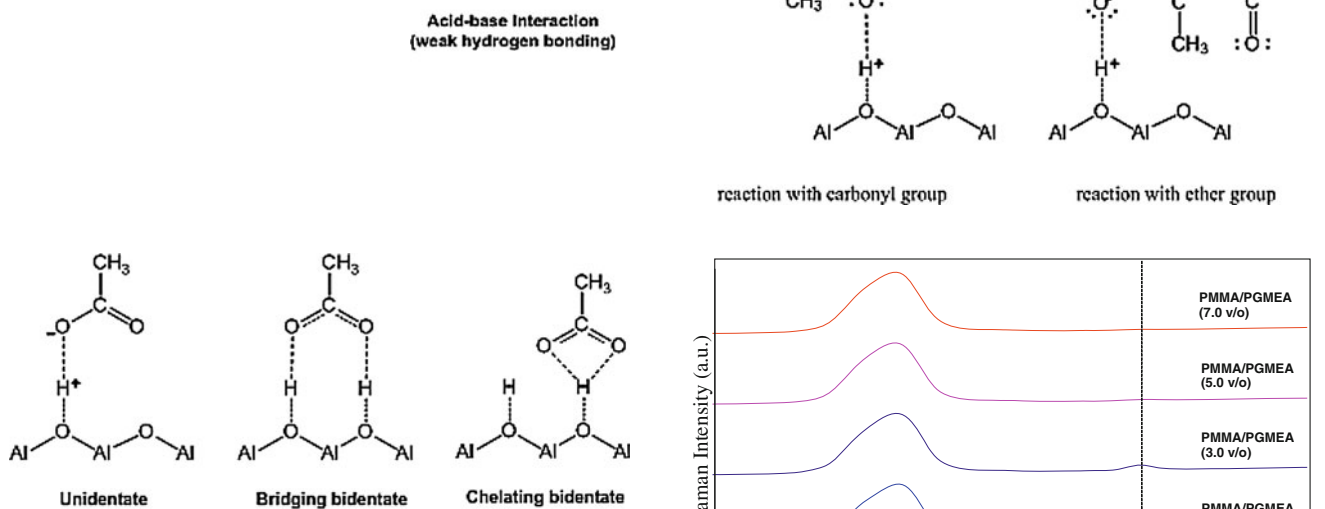


Fig. 1 ATR–FTIR spectra of PGMEA, bound PGMEA, and aluminum oxide

Scheme 1 Acid–base interaction between PGMEA and aluminum oxide particle



Scheme 2 Ionic binding structures acetate anion and aluminum oxide surface

and 1730 cm^{-1} , respectively. The relative peak intensity of the unpolymerized and the polymerized PMMA is illustrated in Fig. 2. The peak intensity ratio between $\text{C}=\text{C}/\text{C}=\text{O}$ was used as the indicator of extent of polymerization [28]. In addition, the degree of conversion (DC%) can be calculated by comparison of the area (A) ratio prior to and after polymerization reaction as shown below [16, 17].

$$\text{Degree of conversion (\%)} = \left(1 - \frac{(\text{A}_{\text{C}=\text{C}}/\text{A}_{\text{C}=\text{O}})_{\text{polymersized}}}{(\text{A}_{\text{C}=\text{C}}/\text{A}_{\text{C}=\text{O}})_{\text{unpolymerized}}} \right) \times 100.$$

Since the PGMEA was introduced along with the nanoparticles, the effect of the glycol molecule on degree of conversion was first examined. The relative Raman peak

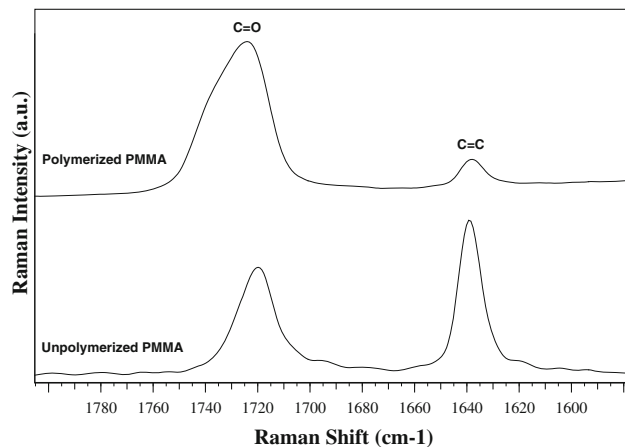


Fig. 2 Raman spectra of polymerized and unpolymerized PMMA

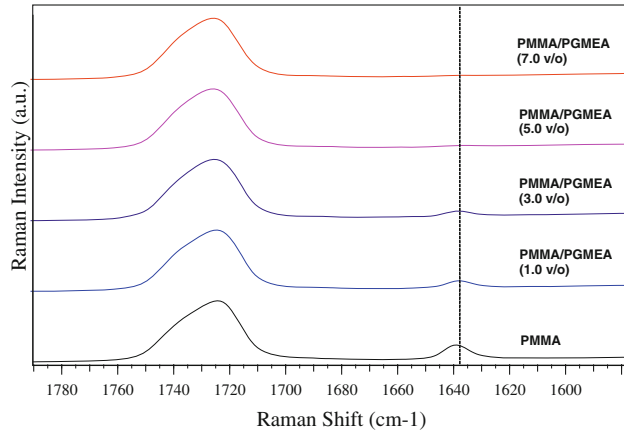


Fig. 3 Raman spectra of PMMA/PGMEA composites

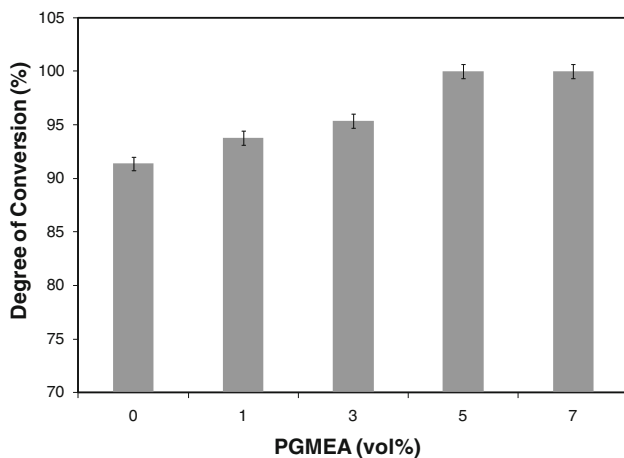


Fig. 4 Effect of PGMEA on degree of conversion (%)

intensities between $\text{C}=\text{O}$ and $\text{C}=\text{C}$ and degree of monomer conversion of difference PGMEA addition are shown in Figs. 3 and 4, respectively. The degree of monomer conversion achieved is as great as 91.37% in the neat PMMA system and is further enhanced with glycol additions. Virtually complete polymerization is obtained when the glycol content reaches 5.0 v/o. Diffusivity of species in the material significantly influences polymerization process [30]. Free volume is a key parameter related to molecular

diffusion and the monomer conversion process [31]. In this sense, PGMEA additions increase the total free volume and enhance the diffusivity of the reactive species which leads to greater levels of polymerization. The decrease in glass transition temperature (T_g) with increasing PGMEA [32] further adds to the increasing overall level of free volume.

Nanoparticles can typically be incorporated into polymer matrices in two ways—to the monomer prior to polymerization (*in situ*) and to the polymer by melt blending or other methods (*ex situ*). In the case of *in situ* polymerization, the added nanoparticles have been reported to influence the degree of polymerization. For example, the addition of silver nanoparticles during suspension polymerization of PMMA slightly lowered the rate of polymerization and degree of polymerization as compared to the neat system, presumably as a result of radical absorption by silver nanoparticles [33]. The *in situ* polymerization of nanocomposites presented in this work revealed that the nanoparticles influenced the degree of conversion of PMMA as shown in Figs. 5 and 6 for 45 and 20 nm aluminum oxide, respectively. In the system containing dry-aluminum oxide (dashed line B), the degree of conversion was 85% which corresponds to a 6% decrement as compared to the neat PMMA (dotted line A). However, the percent conversion *increases* with the addition of predispersed (functionalized) aluminum oxide nanoparticles of either size, which is explained by the surface-adsorbed PGMEA. With regard to specific particle size effects, two competing factors are in play here that we have not fully resolved. Smaller particles are expected to have a greater effect than larger particles in *reducing* the conversion extent as discussed previously for nanoparticles in general. However, the smaller (20 nm) particles used in this study were also associated with higher levels of PGMEA (in part due to their higher surface-area-to-volume ratio) which has

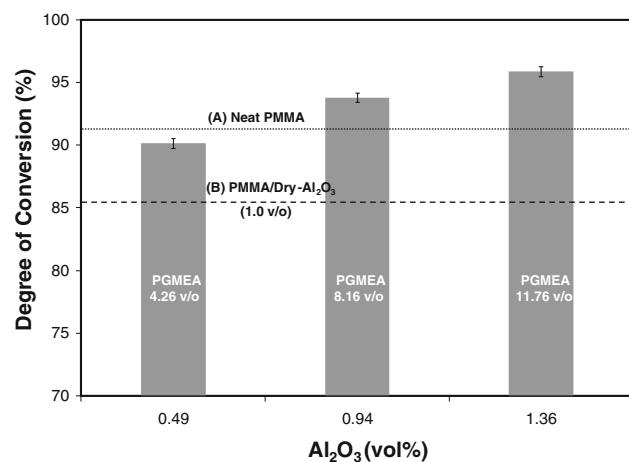


Fig. 6 Effect of FG-Al₂O₃ particles (20 nm) on the degree of conversion (%) at various nanoparticle volume fractions

been shown to *increase* the conversion. Overall, the net effect is that the conversions shown in Fig. 6 are slightly greater than those in Fig. 5, indicating that the conversion enhancing effect of higher PGMEA levels is greater than the conversion inhibiting effects of smaller particle size.

Summary

Nanocomposites of PMMA and aluminum oxide were examined with respect to the molecular structure of the interfacial region between polymer and particle. Both acid–base interaction and complex structures of absorbed species (PGMEA and PMMA) were confirmed to form at the metal oxide surface through secondary bonding. The hydrogen bonding results in a red shift of the carbonyl stretching and ether stretching peaks. Both unidentate and bidentate complex structures were identified in the infrared spectrum.

Raman spectroscopy was used to investigate the degree of monomer conversion. The metal oxide surface has the ability to absorb free radicals during the polymerization process, which results in 6% reduction of monomer conversion in the PMMA/dry-aluminum oxide as compared to the neat PMMA. On the other hand, the percent conversion is enhanced when the oxide is introduced in the form of functionalized nanoparticles. In the PMMA/dry-aluminum oxide system, the particle surface is highly active and strongly chemisorbs the radical species, whereas in the PGMEA–aluminum oxide system the majority of particle surface is covered by the glycol and hence the probability of radical absorption is reduced.

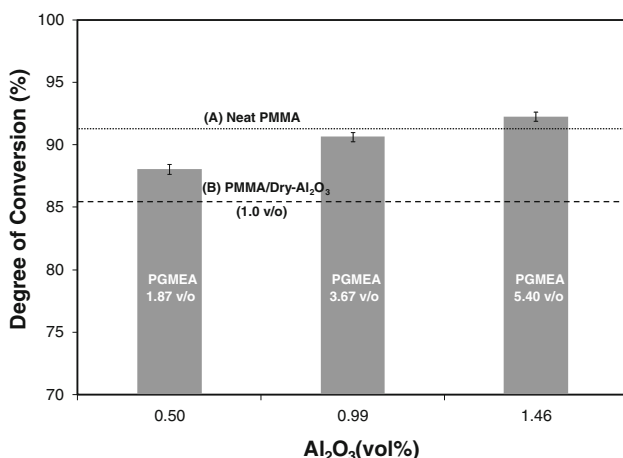


Fig. 5 Effect of FG-Al₂O₃ particles (45 nm) on the degree of conversion (%) at various nanoparticle volume fractions

Acknowledgements We thank the AMIPP Advanced Polymer Center for sponsoring this work, and the assistance of Professor Gene Hall in the area of ATR-FTIR was essential to this article.

References

1. Rong MZ, Zhang MQ, Zheng YX, Zeng HM, Walter R, Friedrich K (2001) *Polymer* 42:167
2. Rong MZ, Ji QL, Zhang MQ, Friedrich K (2002) *Euro Polym J* 38:1573
3. Chan C-M, Wu J, Li J-X, Cheung Y-K (2002) *Polymer* 43:2981
4. Reynaud E, Jouen T, Gauthier C, Vigier G, Varlet J (2001) *Polymer* 42:8759
5. Jordan J, Jacob KI, Tannenbaum R, Sharaf MA, Jasiuk I (2005) *J Mater Sci Eng* 393:1
6. Choi J-H, Jung C-H, Kim D-K, Suh D-H, Nho Y-C, Kang P-H, Ganeshan R (2009) *Radiat Phys chem* 78:517
7. Kyu T, Zhou ZL, Zhu GC, Tajuddin Y, Qutubuddin S (1996) *J Polym Sci B Polym Phys* 34:1761
8. Rasmussen WL (2001) Ph.D. dissertation, Virginia Polytechnic Institute and State University
9. Radicevic R, Stojkovic DM, Budinski-Simendic J (2000) *J Therm Anal Calorim* 62:237
10. Pallikari-Viras F, Li X, King TA (1996) *J Sol-Gel Sci Tech* 7:203
11. Inchausti I, Sasia PM, Katime I (2005) *J Mater Sci* 40:4833. doi: [10.1007/s10853-005-2003-y](https://doi.org/10.1007/s10853-005-2003-y)
12. Motokawa R, Nakahira T, Annaka M, Hashimoto T, Koizumi S (2004) *Polymer* 45:9019
13. Abdollahi M, Sharifpour M (2007) *Polymer* 48:25
14. Guerra RM, Duran I, Ortiz P (1996) *J Oral Rehabil* 23:632–637
15. Miyazaki M, Onose H, Iida N, Kazama H (2003) *Dent Mater* 19:245
16. Khalil SKH, Allam MA, Tawfik WA (2007) *Eur J Dentist* 1:72
17. Pianelli C, Devaux J, Bebelman S, Leloup G (1999) *J Biomed Mater Res* 48:675
18. Rehman I, Harper EJ, Bonfield W (1996) *Biomaterials* 17:1615
19. Hagan CP, Orr JF, Mitchell CA, Dunne NJ (2009) *J Mater Sci Mater Med* 20:2427
20. Kondo T (1997) *Cellulose* 4:281
21. Grohens Y, Schultz J, Prud'homme RE (1997) *Int J Adhesion Adhesive* 17:163
22. Kulkeratiyut S, Kulkeratiyut S, Blum FD (2006) *J Polym Sci B Polym Phys* 44:2071
23. Tao W, Fei F, Yue-Chuan W (2006) *Polym Bull* 56:413
24. Khaled SM, Rizkalla AS, Charpentier PA (2008) AIChE Conference proceeding at Philadelphia, PA
25. Du X-W, Fu Y-S, Sun J, Han X, Liu J (2006) *Semicond Sci Technol* 21:1202
26. Nara M, Torii H, Tasumi M (1996) *J Phys Chem* 100:19812
27. Galin MA, Turkish L, Chowchuvech E (1977) *Am J Ophthalmol* 84:153
28. Pallikari F, Chondrokoukis G, Rebelakis M, Kotsalas Y (2001) *Mater Res Innov* 4:89
29. Kantarci Z, Aksoy S, Hasirci N (1997) *Int J Artif Organs* 20:407
30. Sideridou I, Tserki V, Papanastasiou G (2002) *Biomaterials* 23:1819
31. Elliott JE, Lovell LG, Bowman CN (2001) *Dental Mater* 17:221
32. Viratyaporn W, Lehman R (2010) *J Thermal Anal Calorim* (submitted)
33. Yeum J-H, Deng Y (2005) *Colloid Polym Sci* 283:1172